J|A|C|S
ARTICLES
Published on Web 07/03/2004

Interfacial Nano-structuring of Designed Peptides Regulated by Solution pH

Jian R. Lu,[†] Shiamalee Perumal,[†] Ian Hopkinson,[†] John R. P. Webster,[‡] Jeff Penfold,[‡] Wonmuk Hwang,[§] and Shuguang Zhang[§]

Contribution from the Biological Physics Group, Department of Physics, UMIST, PO Box 88, Manchester M60 1QD United Kingdom, Centre for Biomedical Engineering NE47-379, Massachusetts Institute of Technology, 77 Massachusetts Avenue, Cambridge, Massachusetts 02139-4307, and ISIS Neutron Facility, CLRC, Rutherford Appleton Laboratory, Chilton, Didcot OX11 0QZ, United Kingdom

Received January 29, 2004; E-mail: j.lu@umist.ac.uk

Abstract: The in-situ conformations of peptide layers formed from the adsorption of two different synthetic 15-mer peptides at the hydrophilic silicon oxide/aqueous solution interface have been determined using neutron reflectivity (NR). The first peptide is based on the native sequence of a protein-binding domain within a heteromeric transcriptional activator, HAP2, identified from yeast *Saccharomyces cerevisiae*, with tyrosine (Y) present at the 1st, 8th and 15th amino acid positions, hence we denote this YYY15. Substitution of tryptophan (W) at the same locations gives WWW15. Both peptides have α-helical structure in phosphate buffer, as determined by circular dichroism (CD) spectra. D_2O was used as solvent in the NR experiments to highlight structural heterogeneity across the hydrogenated peptide layers. At pH 7, YYY15 was found to form a weakly adsorbed interfacial monolayer. However, the mutant WWW15 showed strong interfacial adsorption, with the interfacial layer characterized by a middle hydrophobic sublayer of 7−8 Å with lower scattering length density and two almost symmetrical hydrophilic outer sublayers of 6−8 Å with higher scattering length density, suggesting the formation of a "sideways-on" helical conformation. An increase in pH to 9 resulted in the improved packing within the interfacial layer with similar structure. However, decrease in pH to 5 reduced the interfacial adsorption, mainly due to the enhanced solubility of the peptides associated with the protonation of arginine (R) and lysine (K) groups and the decreasing concentration of divalent HPO_4^{2-} in the phosphate buffer. Subsequent assessment of the reversibility of adsorption showed that once the peptide layers were formed they did not desorb. These interfacial structures may provide feasible routes to interfacial nano-templating.

Introduction

The self-assembly of short synthetic peptides (<50 amino acids), into molecular nano-structures is attracting growing interest in nano-biotechnology. The use of the secondary structural elements of proteins, i.e., α-helices, β-sheets, turns, β-helices and loops to engineer molecular arrangements amenable to the design of predictable and functional nano-structures has been extensively explored using synthetic peptides with different sequences and molecular structures. These activities represent the bottom-up approach of mimicry to the self-assembly observed in biology to fabricate supramolecular structures from designed peptides.

Zhang et al.[1−4] discovered and reported several classes of ionic self-complementary peptides that self-assemble spontaneously to form interwoven nano-fibers, which formed hydrogels consisting of greater than 99% water. These peptides are surfactant-like and they are characterized by well-defined hydrophilic and hydrophobic moieties. The introduction of charge modulation makes them resemble block copolymers. The structure of these hydrogels is believed to consist of a small scale structure of self-assembled peptides which then, in turn, assemble to form a network. This type of sequence has a tendency to form stable β-sheet structure in water and they can serve as ideal scaffolds for tissue-cell attachment, extensive neurite outgrowth, and formation of active nerve connections.

Aggeli et al.[5,6] have shown that short peptides of different structural origins could also form long, semi-flexible, polymeric β-sheet peptide nano-tapes in nonaqueous medium, indicating the intrinsic nature of self-assembly of peptides as a potential route to novel biomaterials. In another study by Ghadiri et al.,[7,8]

[†] Biological Physics Group, Department of Physics, UMIST.
[‡] Centre for Biomedical Engineering NE47-379, Massachusetts Institute of Technology.
[§] ISIS Neutron Facility, CLRC, Rutherford Appleton Laboratory.

(1) Zhang, S.; Holmes, T.; Lockshin, C.; Rich, A. *Proc. Natl. Acad. Sci. U.S.A.* **1993**, *91*, 1345.
(2) Holmes, T. C.; De Lecalle, S.; Su, X.; Liu, G.; Rich, A.; Zhang, S. *Proc. Natl. Acad. Sci. U.S.A.* **2000**, *97*, 6728.
(3) Caplan, M.; Moore, P.; Zhang, S.; Kamm, R. D.; Lauffenburger, D. A. *Biomacromolecules* **2001**, *4*, 627.
(4) Vauthey, S.; Santoso, S.; Gong, H.; Watson, N.; Zhang, S. *Proc. Natl. Acad. Sci. U.S.A.* **2002**, *99*, 5355.
(5) Aggeli, A.; Nyrkova, I. A.; Bell, M.; Harding R.; Carrick, L.; McLeish, T. C. B.; Semenov, A. N.; Boden, N. *Proc. Natl. Acad. Sci. U.S.A.* **2001**, *98*, 11 857.
(6) Aggeli, A.; Bell, M.; Boden, N.; Keen, J. N.; Knowles, P. F.; McLeish, T. C. B.; Pitkealthy, M.; Radford, S. E. *Nature* **1997**, *386*, 259.

10.1021/ja049477r CCC: $27.50

D,L- α-peptides and cyclic β-peptides were shown to produce flat, ring-shaped self-assembling nano-tubes with diameter around 1 nm in the single peptide tube. These peptide nanotubes were also shown to form pores in the cell membrane.

Tirrell's group[9] demonstrated that synthetic proteins prepared using recombinant DNA methods self-assemble in bulk solution to form nano-assemblies, with the nano-structuring and subsequent gel formation being tunable to solution pH and temperature. Gore et al. then showed that similar micellar aggregation and the gelation process could be mimicked by short peptides bearing single and double hydrophobic tails.[10] These peptides have basic molecular structures resembling well-characterized surfactants, but the molecular characteristics of these peptide amphiphiles bring new features that surpass traditional surfactants. More recently, Stupp's group[11,12] has elegantly demonstrated that peptide amphiphiles bearing different sequences and alkyl tail can also self-assemble and form viscous gel phases, and that the processes are responsive to pH shift, divalent ion induction and solution concentration. These authors also showed that modification in the hydrophobic alkyl tails produced nanofibers of varying morphology.

We have recently explored the structural features of peptide layers formed at the solid/aqueous solution interface. Interfacial self-assembly of short peptides leads to the formation of interfacial layers of different structural characteristics. These structural features are potentially attractive for applications such as nano-sensors and nano-circuits. The amphiphilic nature of synthetic peptides tends to lead to their interfacial adsorption, driven by electrostatic and hydrophobic forces, hydrogen bonding and entropic effects. Because interfaces represent different energetic balances from bulk solution, peptides self-assembled at planar interfaces may adopt different structural conformations.[13−16] To realize the potential afforded by peptide interfacial assembly, it is important to be able to control the structure and morphology of the peptide layers formed at the interfaces. Understanding the effects of primary sequence and solution conditions on the structural properties of surface layers constitute an essential step toward the improved fundamental understanding necessary for developing the applications of peptide interfacial layers.

Neutron reflectivity (NR) is a powerful tool for obtaining in situ structural information about an interfacial layer adsorbed at the solid/water interface. NR determines the nuclear scattering length density profile normal to the interface. In previous studies,[17−25] we showed that neutron reflection is capable of simultaneous measurement of the thickness and volume fraction of any protein layer in a direction along the surface normal, with depth resolution at the level of 1−2 Å. This high depth resolution, together with the three-dimensional structural information, allows us to assess the structural orientations of protein molecules at a given surface and solution conditions and to determine the extent of deformation and structural unfolding of globular proteins. Peptides of small and intermediate lengths may be predisposed to forming α-helices or β-sheets at the interface. These transitions can be strongly affected by surface and solution environment, resulting in a different surface layer thickness and packing density, from which further detailed structural projections and orientations within the peptide layer can be inferred.

Scheme 1 Primary Sequences of YYY15 and WWW15

YYY (wild type)

162	164	166	168	170	172	174	176
Y	V	N	A	K	Q	Y	Y
		+		+		+	+

R	I	L	K	R	R	Y
			+	+	+	

WWW15 (mutant)

162	164	166	168	170	172	174	176
W	V	N	A	K	Q	Y	W
		+		+		+	+

R	I	L	K	R	R	W
			+	+	+	

The 15-mer peptides used in this work were derived from a protein-binding domain within a heteromeric transcriptional activator, HAP2, identified from yeast *Saccharomyces cerevisiae*.[26] HAP2 is a 265 amino acid subunit that contains a highly conserved 20 amino acid core which is implicated in subunit assembly. Previous work has demonstrated that a 15-mer synthetic peptide replicating the sequence between positions 162 and 176 in HAP2, showed a typical α-helical circular dichroism (CD) spectrum.[27] The exact sequence for this truncated peptide is shown in Scheme 1.

Figure 1 shows side and end views of α-helical and β-sheet conformations for YYY15. In the α-helical conformation the tyrosine residues at positions 1, 8 and 15 form a "stack", in which interresidue interactions contribute to helical stability. Similar "stacking" of adjacent hydrophobic residues, alanine and leucine, and the interactions of the butylene moieties of two lysines contribute strongly to the formation of stable α-helical structure as revealed by CD. The locations of the three positively charged arginine residues are also marked in Figure 1. As the solid substrate studied in this work was SiO_2, which has a weak negative charge, the positively charge groups provide an essential driving force for interfacial adsorption.

Substitution of tyrosine(Y) with tryptophan(W) at positions 1, 8, and 15 is likely to change the delicate balance of helical stability of the peptides, resulting in different extent of peptide adsorption at the solid SiO_2/water interface. The neutron

(7) Ghadiri, M. R.; Granja, J. R.; Buehler, L. K. *Nature* **1994**, *369*, 301.
(8) Bong, D. T.; Clark, T. D.; Granja, J. R.; Ghadiri, M. R. *Angew. Chem., Int. Ed. Engl.* **2001**, *40*, 988.
(9) Petka, W. A.; Harden, J. L.; McGrath, K. P.; Wirtz, D.; Tirrell, D. A. *Science* **1998**, *281*, 389.
(10) Gore, T.; Dori, Y.; Talmon, Y.; Tirrell M.; Bianco-Peled, H. *Langmuir* **2001**, *17*, 5352.
(11) Hartgerink, J. D.; Beniash, E.; Stupp S. I. *Science* **2001**, *294*, 1684.
(12) Hartgerink, J. D.; Beniash, E.; Stupp, S. I. *Proc. Natl. Acad. Sci. U.S.A.* **2002**, *99*, 5133.
(13) Rapaport, H.; Kjaer, K.; Jensen, T. R.; Leiserowitz, L.; Tirrell, D. A. *J. Am. Chem. Soc.* **2000**, *122*, 12 523.
(14) Powers, E. T.; Kelly, J. W. *J. Am. Chem. Soc.* **2001**, *123*, 775.
(15) Powers, E. T.; Yang, S. I.; Lieber, C. M.; Kelly, J. W. *Angew. Chem., Int. Ed.* **2002**, *41*, 127.
(16) Lu, J. R.; Perumal, S.; Powers, E.; Kelly, J.; Webster, J.; Penfold, J. *J. Am. Chem. Soc.* **2003**, *125*, 3751.
(17) Lu, J. R.; Su, T. J.; Thomas, R. K.; Penfold, J.; Webster, J. *J. Chem. Soc., Faraday Trans.* **1998**, *94*, 3279.
(18) Lu, J. R.; Su, T. J.; Howlin, B. *J. Phys. Chem. B* **1999**, *103*, 5903.
(19) Su, T. J.; Lu, J. R.; Thomas, R. K.; Cui, Z. F. *J. Phys. Chem. B* **1999**, *103*, 3727.
(20) Su, T. J.; Green, R. J.; Wang, Y.; Murphy, E. F.; Lu, J. R.; Ivkov, R.; Satija, S. K. *Langmuir* **2000**, *16*, 4999.
(21) Lu, J. R.; Su, T. J.; Penfold, J. *Langmuir* **1999**, *15*, 6975.
(22) Su, T. J.; Lu, J. R.; Thomas, R. K.; Cui, Z. F.; Penfold, J. *J. Phys. Chem. B* **1998**, *102*, 8100.
(23) Lu, J. R.; Su, T. J.; Thomas, R. K.; Rennie, A. R.; Cubit, R. *J. Colloid Interface Sci.* **1998**, *206*, 212.
(24) Lu, J. R.; Lee, E. M.; Thomas, R. K. *Acta Crystallogr.* **1996**, *A52*, 11.
(25) Lu, J. R.; Thomas, R. K. *J. Chem. Soc., Faraday Trans.* **1998**, *94*, 995.
(26) Xing, Y.; Zhang, S.; Olesen, J. T.; Rich, A.; Guarente, L. *Proc. Natl. Acad. Sci. U.S.A.* **1994**, *91*, 3009.
(27) Although the α-helical content is similar in the aqueous solution for the two peptides, adsorption onto the negatively charged SiO_2 surface may induce different extent of disordered structure.

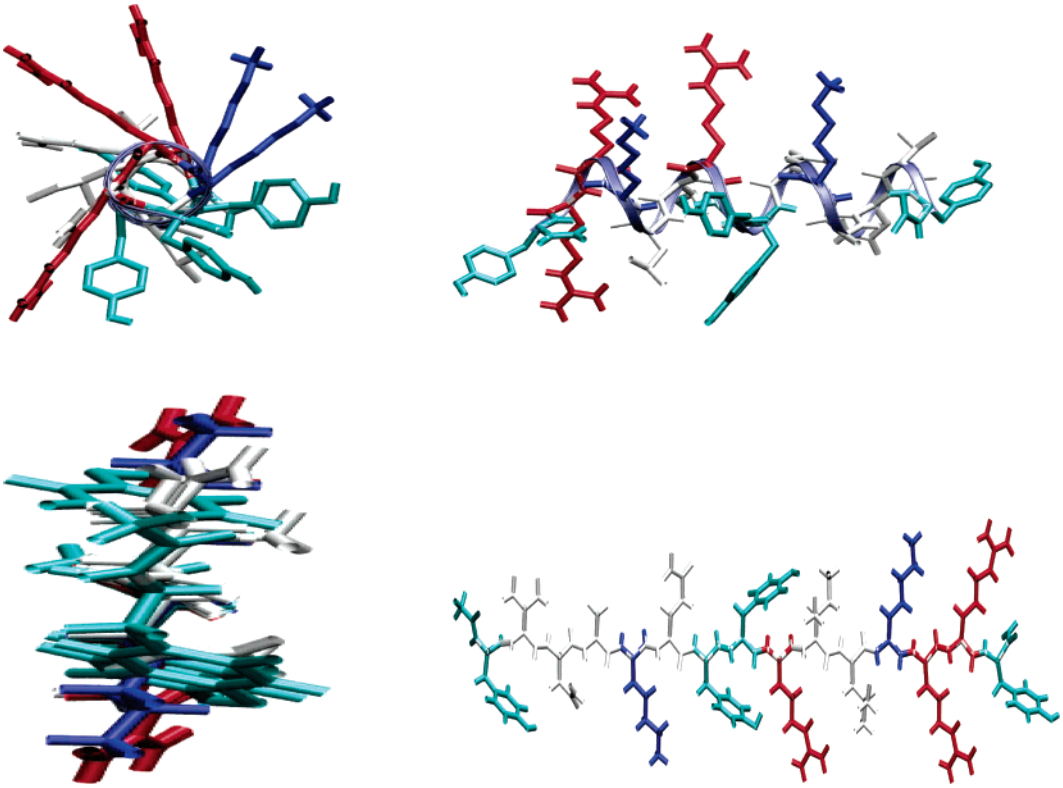

Figure 1. End view (left) and side view (right) of YYY15 in α-helix (top) and *β*-sheet (bottom) conformations. Y groups are shown in cyan, R groups in red and K groups in blue. The helical backbone is represented as a ribbon. Note that several positively charged residues, arganine (R) and lysine (K) are on one side (upper) of the helix and that hydrophobic residues on the other. All molecular models were made using the software VMD.[36]

reflection experiments have shown that the surface layer is a well-packed sideways-on peptide layer at pH 7 and 9 for mutant WWW15, whereas YYY15 shows a rather loose layer packing under the same solution conditions. However, when solution pH is lowered to 5, no adsorption was detected for either of the two peptides. The lack of surface affinity is consistent with the expected increase in peptide hydrophilicity associated with protonation of lysine and arginine groups although increase in the opposite charge density would favor the adsorption. This is in strong contrast to the continued peptide adsorption when the peptide layer preadsorbed at high pH was exposed to low pH solution, indicating the high extent of irreversibility. These structural features are highly relevant to the exploitation of peptide interfacial assembly in nano-biotechnology.

Results

We first compared the relative adsorption of the two peptides, YYY15 and WWW15, by comparing the reflectivity measured with the peptide solution concentration fixed at 0.1 wt % (~5 × 10^{-4} M). The measurements were made at the hydrophilic solid/D_2O interface with the solution pH being fixed at 7 using phosphate buffer. Figure 2 shows the measured reflectivity, $R(\kappa)$, plotted as a function of wave-vector transfer, κ, perpendicular to the reflecting interface

$$\kappa = \frac{4\pi \sin \theta}{\lambda} \qquad (1)$$

where θ is the incidence angle and λ the wavelength of the incidence neutron beam.[29,30] As a control, reflectivity was also measured for a pure D_2O buffer (Figure 2, dashed line). It can be seen from Figure 2 that the adsorption of the YYY15 from solution caused a slight deviation of the reflectivity from the

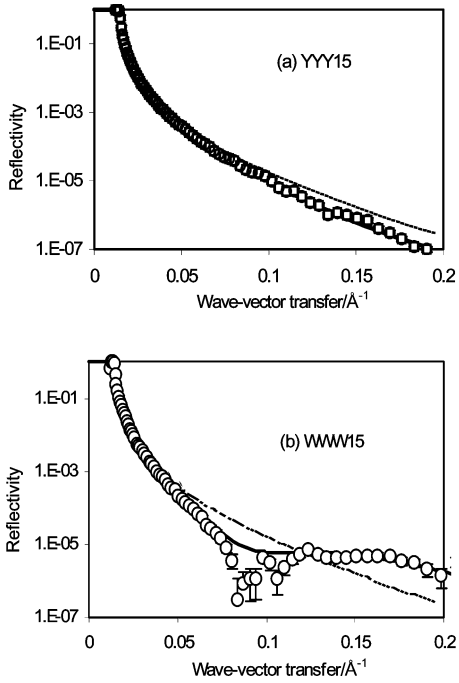

Figure 2. Reflectivity profile measured from the solid SiO_2/D_2O interface (dashed line) is compared with the ones from 0.1 wt % YYY15 (a) and WWW15 (b) at pH 7. The continuous lines represent the best uniform fits with structural parameters listed in Table 1.

(28) Burkett, S. L.; Read, M. J. *Langmuir* **2001**, *17*, 5059. Also: Read, M. J.; Burkett, S. L. *J. Colloid Interface Sci.* **2003**, *261*, 255.

(29) Lu, J. R.; Lee, E. M.; Thomas, R. K. *Acta Crystallogr.* **1996**, *A52*, 11.
(30) Lu, J. R.; Thomas, R. K. *J. Chem. Soc., Faraday Trans.* **1998**, *94*, 995.

pure D_2O profile, indicating a small amount of peptide adsorption. In comparison, adsorption from the WWW15 solution produces a large deviation, notice in particular the relatively strong interference fringe, indicating the presence of a discrete layer with a scattering length density different from that of solution and substrate.

As described previously,[16−25] quantitative information about the thickness and composition of the adsorbed layers can be obtained from model fitting based on the optical matrix formalism. As usual, the modeling process was started with an assumption of a structural model for the adsorbed layer, followed by calculation of the reflectivity from the model. The calculated reflectivity was then compared with the measured data and the structural parameters were then varied in a least-squares iteration until a best fit was found. The structural parameters used in the fitting were the number of layers, thickness (τ), and the corresponding nuclear scattering length density (ρ) for each layer (equivalent to optical refractive index). From the fitted layer data we can derive two further useful parameters; the overall volume fraction of the protein, ϕ_p, in the adsorbed layer

$$\phi_p = \frac{(\rho - \rho_w)}{(\rho_p - \rho_w)} \tag{2}$$

where ρ_w is the scattering length density of D_2O ($= 6.35 \times 10^{-6}$ Å^{-2}), ρ_p is the scattering length density of the protein ($= 3.47 \times 10^{-6}$ Å^{-2} for YYY15 and 3.55×10^{-6} Å^{-2} for WWW15) and ρ is the fitted scattering length density. For a multilayer fit the weighted average scattering length density for the layers will give an overall volume fraction for the entire absorbed layer.

The second parameter which we can derive is the area per molecule, A, of the peptide

$$A = \frac{V_p}{\sum \phi_p \tau_i} \tag{3}$$

where V_p is the molecular volume of the appropriate peptide (2540 Å^3 for YYY15 and 2525 Å^3 for WWW15). The sum is over all the layers in the model.

The model fitting of the measured reflectivity in pure D_2O buffer resulted in a SiO_2 layer of 15 Å with $\rho = 3.4 \times 10^{-6}$ Å^{-2}, this is identical to the value for amorphous SiO_2, thus showing that the oxide layer is smooth and is free of defects and voids. The presence of any defects, which would be filled by D_2O, would result in a greater value of ρ for the layer. In all of models which follow, this oxide layer is included. The subsequent model fitting to the 0.1 wt % YYY15 reflectivity shown in Figure 2a was carried out assuming that the peptide formed a single, uniform layer when adsorbed onto the oxide layer surface. The best single layer fit, as shown in Figure 2a, gave a thickness of 26 Å with $\rho = 5.8 \times 10^{-6}$ Å^{-2}. Using eq 2 we can see that this corresponds to a volume fraction of the peptide in the layer, $\phi_p = 0.19$ and from eq 3 we find an area per molecule of 512 Å^2.

Data from a layer absorbed from 0.1 wt % WWW15 was not fitted well by a single layer model, this indicates that the scattering length density distribution within the monolayer is not uniform in a direction normal to the surface. Subsequent attempts to adopt a two-layer model did not produce any

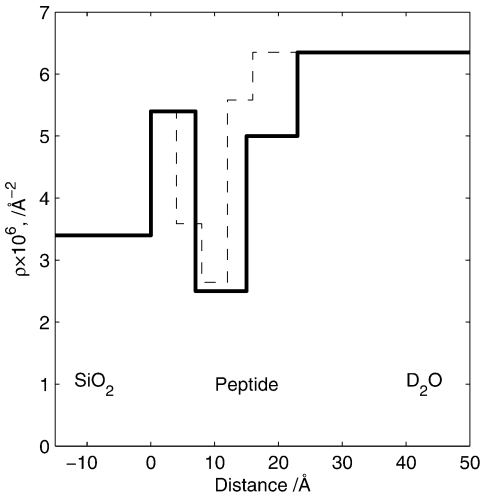

Figure 3. Measured scattering length density profile, $\rho(z)$, for WWW15 at 0.1 wt % and pH 7(solid line) and calculated for an adsorbed WWW15 in α-helical conformation (broken line).

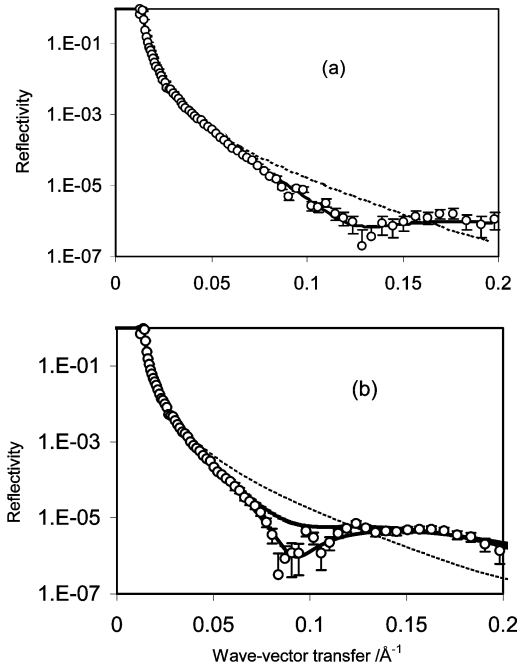

Figure 4. Neutron reflectivity measured from peptide WWW15 adsorbed at the SiO_2/D_2O interface with the peptide concentration at 0.01 (a) and 0.1 wt % (b). The reflectivity from the pH 7 D_2O buffer is shown as dashed line for comparison. The continuous lines represent the best uniform layer fit in (a) and three layer model fit in (b). The long dashed line in (b) represents the best uniform layer fit.

satisfactory fit to the measured reflectivity either. A three-layer model was able to fit the experimental data. The continuous line shown in Figure 4b represents the best three layer fit to 0.1 wt % WWW15 reflectivity profile, with the resulting structural parameters listed in Table 1, which summarizes all the model fit parameters used in this work. A comparison of the measured scattering length density profile, $\rho(z)$, for WWW15 with the calculated scattering length density profile for a WWW15 molecule in pure α helical form with its long axis parallel to the surface is shown in Figure 3. For the WWW15 model the inner sublayer (τ_1), closest to the oxide surface, was found to be 7 Å thick. This value was very close to the thickness of 8 Å of the outer sublayer, indicating a high degree of

Table 1. Structural Parameters Obtained for Fits to Neutron Reflectivity Data from Peptide Layers Adsorbed under a Range of Conditions

	wt %	pH	parameter	layer 1	layer 2	layer 3	ϕ_P
YYY15	0.01	7	$\tau \pm 2$/Å	16			0.25
			$(\rho \pm 0.2) \times 10^6$/Å^{-2}	5.62			
YYY15	0.1	7	$\tau \pm 2$/Å	26			0.19
			$(\rho \pm 0.2) \times 10^6$/Å^{-2}	5.8			
WWW15	0.001	7	$\tau \pm 2$/Å	12			0.73
			$(\rho \pm 0.2) \times 10^6$/Å^{-2}	4.3			
WWW15	0.01	7	$\tau \pm 2$/Å	13			0.84
			$(\rho \pm 0.2) \times 10^6$/Å^{-2}	4.0			
WWW15	0.1	7	$\tau \pm 2$/Å	7	8	8	0.75
			$(\rho \pm 0.2) \times 10^6$/Å^{-2}	5.4	2.5	5.0	
WWW15	0.1	9	$\tau \pm 2$/Å	8	9	10	0.76
			$(\rho \pm 0.2) \times 10^6$/Å^{-2}	5.4	2.3	5.0	

structural symmetry. The high ρ values for the two side sublayers indicated a high volume fraction of water within the side chain amino acid region. In contrast, the thickness of the middle sublayer is also 7−8 Å, and its scattering length density was very low, indicating very low water content and a comparatively high peptide packing density. Other possible three layer models, e.g., with a higher scattering length density in the middle sublayer, were found not to fit the data at all and were thus ruled out from the model testing. The calculated profile for WWW15 has the same features as the experimentally measured profile with a core of low scattering length density; the regions of higher scattering length density are somewhat thinner in the simulation. There are a number of possible reasons for this; the structure coordinates for WWW15 were minimized "in vacuo"; the D_2O was added to the calculated system in a crude way which does not allow for the finite volume of the D_2O molecules. Furthermore, we expect the peptide in the experimental system to be more disordered.

The three layer model fit to the WWW15 data indicates a total layer thickness of 23Å and an area per molecule of 147 Å^2, which is equivalent to an overall protein volume fraction, $\phi_p = 0.75$. Therefore, while the total layer thickness (τ) is comparable, the mutated peptide (WWW15) is substantially more surface active than the wild type. The increased adsorption is mainly reflected in the increased peptide volume fraction and hence reduced area per molecule (A).

As WWW15 was more surface active it was selected for the investigation of the variation of adsorption with bulk concentration. The measurements were performed between 0.001% (5×10^{-6} M) and 0.1 wt % (5×10^{-4} M), again at pH 7. As can be seen from Figure 4a, the adsorption from 0.01 wt % WWW15 causes a clear deviation from the pure D_2O reflectivity profile, indicating a small but measurable amount of peptide adsorption. However, increase in the peptide concentration to 0.1 wt % sharpens the interference fringe and shifts to lower κ, indicating a substantially increased amount of adsorption and a thicker layer.

The subsequent fitting to the 0.01 wt % WWW15 reflectivity shown in Figure 4a was carried out, here a single layer model for the peptide layer was found to be sufficient to fit the data. This fit, shown in Figure 4a, gave a total layer thickness of 13 Å with $\rho = 4 \times 10^{-6}$ Å^{-2}, consistent with an area per peptide 226 Å^2, $\phi_p = 0.84$.

The concentration dependent peptide adsorption was also assessed for the wild YYY15. Under similar peptide concentrations, YYY15 produced a much lower amount of adsorption.

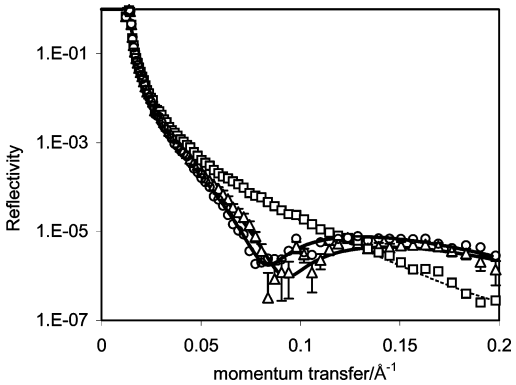

Figure 5. Reflectivity profiles measured at pH 5 (□), 7 (△), and 9 (○) for peptide WWW15. The dashed line represents the reflectivity measured from pure D_2O buffer. The continuous lines are the three layer fits with their structural parameters listed in Table 1.

Both of the peptides listed in Scheme 1 have 2 lysine groups and 3 arginine groups. For the isolated amino acids in bulk solution these groups are positively charged over the pH range 5−9. However, pH shift and surface adsorption may alter the degree of ionization and hence their affinity toward the negatively charged SiO_2 surface. Although increased peptide protonation intuitively makes the peptide more attracted to the SiO_2 surface, it would also increase its solubility, resulting in reduced tendency for interfacial adsorption. In contrast, over the pH 5−9 range the charge density on the SiO_2 surface does not show much variation either.[31] A further factor that should be added to this consideration is the variation of the relative concentrations of NaH_2PO_4 and Na_2HPO_4 with solution pH. In preparing the phosphate buffer (PBS), we have fixed the total PBS molar concentration at 10.7 mM. Thus at pH 7, the molar ratio of $[HPO_4^{-2}]$ to $[H_2PO_4^-]$ is 1.5. This was in contrast to the predominant $H_2PO_4^-$ at pH 5 and HPO_4^{-2} at pH 9. Change in ion composition with pH affected the total ionic strength. Thus the extent of adsorption of the peptide onto the SiO_2 surface is balanced by the fine-tuning of the various interactions involved. Figure 5 compares the reflectivity profiles measured from pH 5, 7 and 9 with the concentration of WWW15 fixed at 0.1 wt %. It can be seen from Figure 5 that the reflectivity profile at pH 5 is virtually identical to the pure D_2O buffer, indicating no peptide adsorption under this condition. This is in contrast to the substantial amount of peptide adsorption at pH 7 as already described above. Further pH shift to 9 results in the increase of peptide adsorption, over and above that attained at pH7, as indicated by the shift of the broad interference fringe to lower κ. These results clearly show a trend of increase in peptide adsorption with the extent of peptide deprotonation and rising divalent ion concentration as described above.

The reflectivity profile obtained at pH 9 can be analyzed quantitatively using a three layer model to represent the peptide layer. The fitted parameters have the same general features as the pH 7 model. Although the total thickness of the peptide layer is slightly larger, at 27 Å, this is a result of a slight increase in the thickness of each of the three layers in the model. The three layer fit is shown by the solid line in Figure 5.

The results presented so far were all obtained at 25 °C, we also measured the adsorption of 0.1 wt % WWW15 at 40 °C and found that the data were best fitted by a three layer model.

(31) Iler, R. K. *The Chemistry of Silica*; Wiley: New York, 1979.

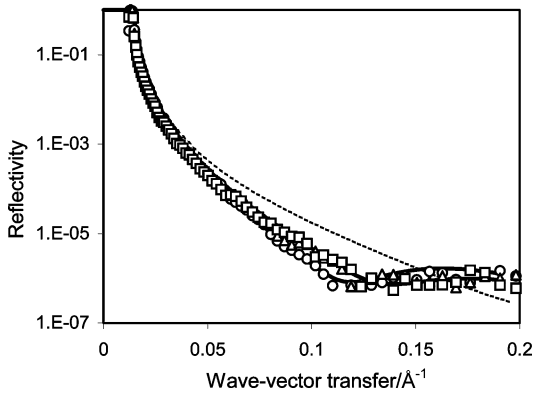

Figure 6. Extent of irreversibility of adsorbed peptide WWW15 as demonstrated by small changes in reflectivity profiles after rinsing under different pH. The peptide layer was adsorbed at pH 7 (○), followed by rinsing with pH 7 buffer (△), and subsequently pH 5 buffer (□) (0.01 wt %). The dashed line represents the reference D_2O measurement.

The overall layer thickness showed a similar layer thickness but there was a slight increase in apparent volume fraction.

The extent of the reversibility of peptide adsorption may have direct implication to their potential applications for interfacial nano-structuring. We examined the extent of desorption by first adsorbing 0.01 wt % WWW15 into the solid/solution interface at pH 7 and then replacing the solution by pH 7 D_2O buffer. Figure 6 shows that the rinsing of the preadsorbed layer by the pure buffer resulted in the removal of some of the adsorbed peptide. The continuous lines shown in Figure 6 represent the best uniform layer fit. It gave $\tau = 14$ Å and $\rho = 3.8 \times 10^{-6}$ Å^{-2} for the preadsorbed layer. After rinsing, $\tau = 11$ Å and $\rho = 3.8 \times 10^{-6}$ Å^{-2}. The results show that the first rinsing reduces the overall layer thickness by some 3 Å, but that further rinsing causes little further desorption. The results also show that the scattering length density remains constant; that most of the preadsorbed peptide remains on the oxide surface after rinsing suggests that the peptide may adsorb sideways-on and that the electrostatic interaction between the positively charged amino acid groups and the negatively charged SiO_2 surface must play an important role. Further exposure of the preadsorbed peptide to sequential rising using pH 5, pH 9 buffers and also 0.5 M NaCl solution did not produce any noticeable variation in the reflectivity.

A similar rinsing procedure was also applied to the WWW15 layer preadsorbed at the high concentration of 0.1 wt % and pH 7. It was found that under this condition little peptide was removed during the same course of rinsing using a combination of pH and salt solution. This increased resistance is likely to be aided by the strong hydrophobic interaction within the middle sublayer.

Discussion

We have found that the adsorption of positively charged peptides onto negatively charged SiO_2 surface is strongly pH dependent. It has been shown that WWW15 adsorption onto the freshly prepared SiO_2 surface results in the maximum at pH 9. As the solution pH becomes more acidic the adsorbed amount drops and at pH 5, there was no adsorption detectable. As already indicated, the pK_a values for the two positively charged amino acids are between 10 and 12. Shift in pH toward acidic condition would be expected to increase positive charges on the peptide and the subsequent increase in attraction to the solid surface, resulting in increased adsorption. At the same time, changes in solution pH over this range is not expected to alter the weakly negative charge density on the SiO_2 surface, although there must be some extent of neutralization between the peptide and the surface. However, the electrostatic interaction between peptide and surface is likely to be counterbalanced by other factors, such as the increased hydrophilicity associated with peptide charge dissociation. That the observed trend is contrary to the strength of this electrostatic interaction, indicates that the dominant effects in this case must be the peptide hydrophilicity and the concentration of divalent ions as outlined previously. This observation emphasizes the need to make in situ adsorption measurements.

The appropriate fitting of uniform layer model for the adsorbed WWW15 layers at the low peptide concentrations indicated that little structural inhomogeneity was detected along the surface normal direction. This observation together with the average thickness of some 12−13 Å suggests that the whole peptide molecules adsorbed sideways-on. The overall structural parameters obtained show that the peptides are unlikely to form head-on adsorption as in the case of surfactants. It is possible that the adsorbed layer consists of a mixture of conformations. If there was a sufficient fraction of head-on adsorption (e.g., greater than 10%) in a predominantly sideways-on conformation, then a diffuse sublayer would be expected on the solution side and NR would be sufficiently sensitive to detect such a peptide volume fraction distribution. The reflectivity profiles were found to be modeled by uniform layer model well, indicating no detectable amount of head-on adsorption.

Further evidence to support the assignment of sideways-on adsorption under these conditions is the almost complete irreversibility in desorption. These observations are entirely consistent with the opposite charges between the SiO_2 surface and the peptides. Other forces such as hydrogen bonding, entropic effects related to dehydration and rehydration of the interface and peptide, and changes in peptide structural configurations are also important during the peptide nano-structuring at the interface.

The area per molecule for WWW15 at 0.01 wt % and pH 7 is 231 Å^2, giving an average area per amino acid residue of 15 Å^2. It is interesting to comment that this value is very close to 16−17 Å^2 estimated from a crystalline surface peptide monolayer reported by Rapaport et al.[13] Note that the difference of 2 Å^2 is well within the experiment error for NR. In our previous NR study of adsorption of 14-mer hairpin peptides at the air/water interface,[16] the limiting area per molecule was found to be 210−220 Å^2, thus also giving a limiting area per average amino acid ca. 15 Å^2. Both the crystalline surface monolayer studied by Rapaport et al. and our 14-mer hairpin peptide formed surface β-sheet configurations. The comparisons indicate that at the low concentration of 0.01 wt %, WWW15 forms a densely packed peptide monolayer and the packing density of the peptide molecules within the interface is close to that adopted by the β-sheet configuration, although it should be borne in mind that both peptides preferred to form α-helical structures in aqueous environment.

Increasing the concentration of WWW15 to 0.1 wt % at pH 7 and 9 resulted in the formation of peptide layers with an area per molecule around 120 Å^2 and the overall layer thickness around 25 Å. The reduction of A by half of the limiting area

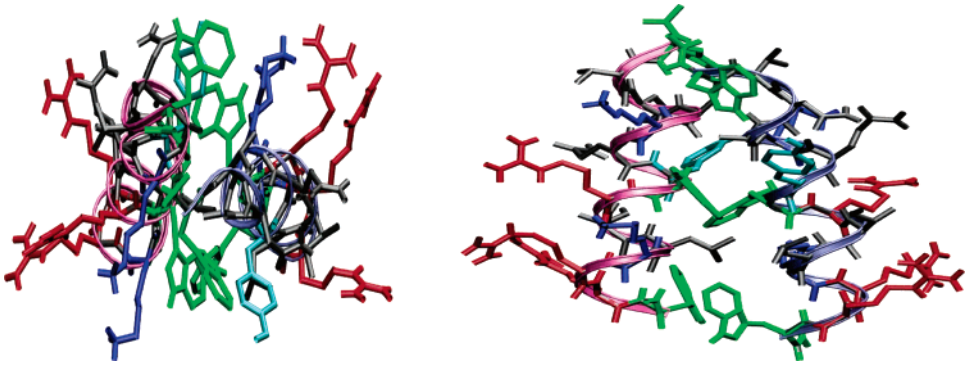

Figure 7. End (left) and side (right) views of a pair of helical−helical configuration held together via the hydrophobic interaction between the three pairs of Ws between them. All the W groups are labeled green and the rest of the color scheme used is the same as in Figure 1.

per molecule necessitated by the single monolayer and the simultaneous increase in layer thickness by almost a factor of 2 suggest that the physically plausible model is the formation of a sideways-on helical adsorption, a different peptide conformation. The sideways-on peptide helical model is also supported from the structural inhomogeneity along the surface normal direction. In fact, the scattering length density for the middle sublayer (ρ_2) at pH 7 was only 2.5×10^{-6} Å^{-2} and was lower than the estimated ρ_p of 3.5×10^{-6} Å^{-2} for the entire peptide. This observation is consistent for our calculations for the scattering length density of the α-helical core region. This structural feature is likely to be aided by either a structural recognition between adjacent WWW or a more general sideways-on peptide packing facilitated by the interdigitation of the hydrophobic sides.

Burkett and Read have performed CD studies on a number of designed peptides adsorbed on negatively charged silicon particles.[28] Their work and the results from protein adsorption studies from other groups[32−34] suggest that surface adsorption generally induces a loss of α-helical structure. Although the CD measurements cannot directly provide specific information on which regions of the molecule interact with the surface, the results have indicated the formation of nonordered structure at the expense of α-helical structure. This trend was especially pronounced for peptides containing arginine groups, which were believed to be the direct anchors on the SiO_2 surface. Burkett and Read also showed that for this type of peptides, there was an increasing extent of transformation from α-helical configuration to nonordered structure with increasing solution pH. We wonder whether there might be a causal link between this increased solution disorder and the higher adsorption we observe at higher pH.

The behavior of WWW15 at low concentrations is consistent with the adsorption of a poorly ordered layer of the peptide. At higher concentrations the almost complete exclusion of water from the central region of the peptide layer suggests close packed configuration enhanced by strong lateral interactions. A plausible scheme for this interaction is the intermolecular stacking of the three tryptophan residues of adjacent peptides, leading to the formation of dimers at the surface. This is illustrated in end and side views in Figure 7. This stacking would produce a hydrophobic core consistent with the observed low scattering length density region. Indirect support for this hypothesis comes from the biological function of the motif from which the peptide originates; it mediates the dimerization of the HAP2 protein. This interaction between tryptophan residues leaves charged residues facing either the substrate or the bulk solution both of which are energetically favored.

In summary, substitution of YYY by WWW has made the latter substantially more surface active. The enhanced surface adsorption may arise from the hydrophobic nature of tryptophan groups and the structural complementarity. The strong adsorption from WWW15 has allowed us to examine the structure and composition of the adsorbed peptide layers with respect to solution pH and peptide concentration in more detail. These changes are summarized in a schematic diagram as shown in Figure 8. In the molecular modeling representation, we assumed that the positively charged groups orient themselves toward the negatively charged SiO_2 surface in the peptide monolayer. In the case of helical formation, the charged groups either point to the SiO_2 surface or into the bulk solution and the hydrophobic groups toward the middle of the pair packing. The thickness of 7−9 Å for the middle layer indicates some degree of interdigitation of the hydrophobic side chains. The side chain segregation is entirely consistent with the variation of scattering length density profile, which indicates a strong water mixing in the inner and outer sublayer but little water in the middle region.

We have shown here that short peptides can effectively adsorb on surfaces to form well ordered structures. Such surface self-assembly phenomenon will be very useful for fabrication of functional nano-coatings that can attract other molecules, cells and a wide range of substance. This functional nano-surface engineering will likely find a broad range of applications that required modified surfaces.[37]

Experimental Section

Neutron reflection experiments were performed at Rutherford Appleton Laboratory near Oxford, UK, using reflectometers CRISP and SURF. The neutron reflectivity profiles were measured at the solid/solution interface using a sample cell and methodology similar to that described in ref 35. The sample cell is a stainless steel trough to which a silicon block is clamped. The neutron beam was defined by four sets of

(32) Billsten, P.; Wahlgren, M.; Arnebrant, T.; McGuire, J.; Elwing, H. *J. Colloid Interface Sci.* **1995**, *175*, 77.
(33) Zoungrana, T.; Findenegg, G. E.; Norde, W. *J. Colloid Interface Sci.* **1997**, *190*, 437.
(34) Kondo, A.; Oku, S.; Higashitani, K. *J. Colloid Interface Sci.* **1991**, *143*, 214.
(35) Lee, E. M.; Thomas, R. K.; Penfold, J.; Ward, R. C. *J. Phys. Chem.* **1989**, *93*, 381.
(36) Humphrey, W.; Dalke, A.; Schulten, K. *J. Mol. Graphics* **1996**, *33*, 14.
(37) Zhang, S. *Nat. Biotechnol.* **2003**, *22*, 1171.

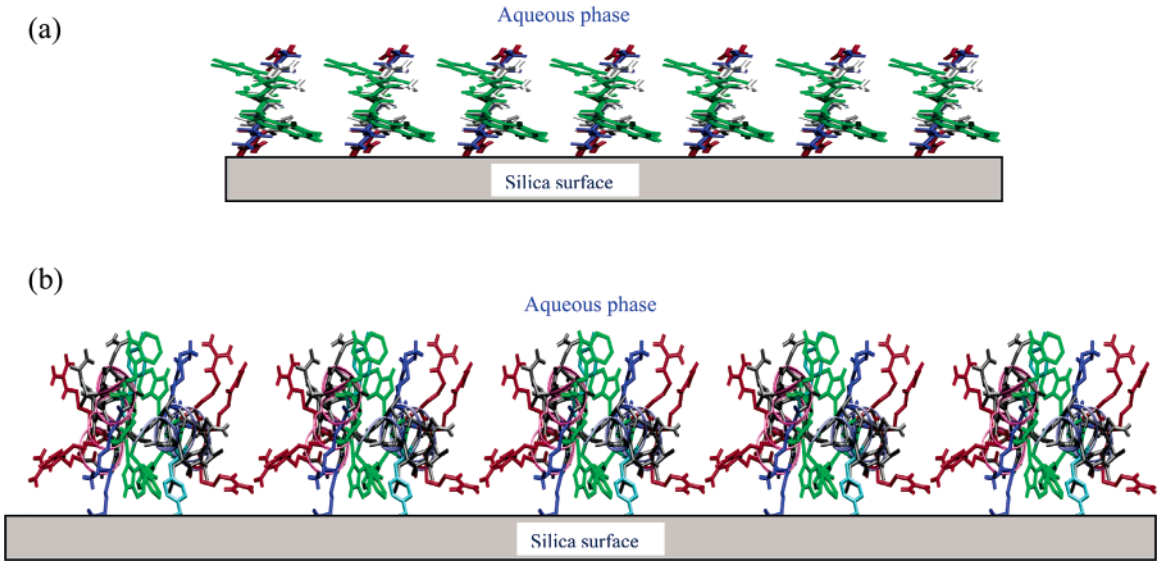

Figure 8. Schematic representations of WWW15 layers adsorbed to a soli/liquid interface (a) at the low concentration of 0.01 wt% and (b) at the high concentration of 0.1 wt %. The solution pH is at 7 or 9. The precise thickness of the layers will depend on how the peptides or peptide pairs orientate themselves with respect to SiO_2 surface.

horizontal and vertical slits placed before the sample container, and is directed such that the beam passes through the silicon block before striking the interface. The beam-illuminated area was typically around 10 × 3 cm, care was taken not to over-illuminate the sample interface. Both reflectometers used white neutron beam with wavelength ranging from 0.5 to 6.5 Å. Each reflection experiment was carried out at three incidence angles of 0.35, 0.8, and 1.8° and the resulting reflectivity profiles combined to cover a wave-vector (κ) range between 0.012 and 0.5 $Å^{-1}$. For the measurements in D_2O, the profiles were scaled so that the reflectivity below the critical angle is 1. For each reflectivity profile, a constant background was subtracted using the average reflectivity between 0.3 and 0.5 $Å^{-1}$.

Prior to the adsorption experiment, the silicon block surface was first polished using diamond emulsions with different particle sizes. The polished silicon block was then rinsed with deionized water. The polished surface was then wiped and rinsed using 5% Decon solution, followed by rinsing with absolute ethanol to remove any residue chemicals and contaminants. Then a Piranha solution composed of 95 parts of concentrated sulfuric acid and 5 parts of hydrogen peroxide solution (29 wt %) was used to clean any further organic traces on the block surface. This was carried out by immersing the Si block in heated Piranha solution at 90 °C for 2 min, followed by rinsing with a large quantity of deionized water. This procedure ensured a consistent hydrophilic block surface, as indicated by the same amount of chicken egg white lysozyme adsorption at 1 gdm^{-3} under pH 7.[19,22]

All peptides were synthesized as C-terminal amides and N-terminal acetylated by standard Fmoc-based solid-phase peptide synthesis (Synpep, Dublin, CA, www.synpep.com). These peptides are HPLC purified and characterized by mass spectroscopy and other standard techniques commercially. The scattering length for each peptide was calculated from the elemental scattering lengths given in ref 38, and the total volume was obtained from addition of volume for each amino acid side chain incorporating the backbone part using the information given in refs 39−41.

The D_2O used was purchased from Sigma and was used as supplied. Its D content was 99.9%. The surface tension at ambient temperature was found to be close to 70 mN/m using Kruss K11 tensiometer. The pH 7 phosphate buffer (PBS) was prepared by fixing NaH_2PO_4 at 4.6 mM and Na_2HPO_4 at 6.1 mM, following the required dissociation equilibrium between different phosphate ions. The pH 5 buffer was obtained by adjusting the pH 7 PBS buffer with a small amount of concentrated HCl (AR grade from Aldrich) and likewise, the pH 9 buffer through the adjustment of a small amount of concentrated NaOH solution (AR from Aldrich). These adjustments did not result in measurable dilution of the total phosphate ion concentrations. However, the total ionic strength varied with pH due to the varying ratio of $H_2PO_4^-$ and $H_2PO_4^{2-}$. Dissolution of peptides into PBS buffer at high concentrations studied tended to lower solution pH by 0.5−1 unit and adjustments were also made by adding an appropriate amount of HCl solution. The final solution pH was checked by a Hanna pH meter (pH 210) before neutron reflection measurements were made.

Acknowledgment. We thank the Engineering and Physical Sciences Research Councils (EPSRC) for funding. S.P. thanks the ISIS Neutron Facility for a CASE studentship.

Note Added after ASAP Publication: In the version published on the Web July 3, 2004, there were errors in Figure 8, errors in the caption to Figure 6, and a few typographical errors. Figure 8, the caption to Figure 6, and the typographical errors have all been corrected in the final Web version published on July 19, 2004 and in the print version.

JA049477R

(38) Sears, V. F. *Neutron News* **1992**, *3*, 26.
(39) Chalikian, T.; Totrov, M.; Abagyan, R.; Breslauer, K. *J. Mol. Biol.* **1996**, *260*, 588.
(40) Stryer, L. *Biochemistry*, 3rd ed.; W. H. Freeman and Company: New York, 1988.
(41) Van Krevelen, D. W. *Properties of Polymers*, 3rd ed.; Elsevier: New York, 1990.